

University of Nebraska - Lincoln

DigitalCommons@University of Nebraska - Lincoln

Faculty Publications in Architectural
Engineering

Durham School of Architectural Engineering
and Construction

Spring 2023

Inter-wythe Slip Design Criteria for Non-Composite Insulated Walls

Abdelrahman Awawdeh

University of Nebraska - Lincoln, aawawdeh2@huskers.unl.edu

Fray F. Pozo-Lora

University of Nebraska - Lincoln, fpozo-lora2@unl.edu

Marc Maguire

University of Nebraska - Lincoln, mmaguire8@unl.edu

Follow this and additional works at: <https://digitalcommons.unl.edu/archengfacpub>



Part of the [Architectural Engineering Commons](#), [Construction Engineering Commons](#), and the [Structural Engineering Commons](#)

Awawdeh, Abdelrahman; Pozo-Lora, Fray F.; and Maguire, Marc, "Inter-wythe Slip Design Criteria for Non-Composite Insulated Walls" (2023). *Faculty Publications in Architectural Engineering*. 204.
<https://digitalcommons.unl.edu/archengfacpub/204>

This Article is brought to you for free and open access by the Durham School of Architectural Engineering and Construction at DigitalCommons@University of Nebraska - Lincoln. It has been accepted for inclusion in Faculty Publications in Architectural Engineering by an authorized administrator of DigitalCommons@University of Nebraska - Lincoln.

1
2
3
4
5
6
7
8
9
10
11
12
13
14
15
16
17
18
19
20
21
22
23
24
25
26
27
28
29
30

INTER-WYTHER SLIP DESIGN CRITERIA FOR NON-COMPOSITE INSULATED WALLS

Abdelrahman Awawdeh, MS, Durham School of Architectural Engineering & Construction
University of Nebraska – Lincoln, Omaha, NE

Fray F. Pozo-Lora, Ph.D., Civil & Environmental Engineering School,
Pontificia Universidad Católica Madre y Maestra, Santo Domingo, Dominican Republic

Marc Maguire, Ph.D., Durham School of Architectural Engineering & Construction
University of Nebraska – Lincoln, Omaha, NE

ABSTRACT

Non-composite insulated wall connector design is governed by ICC-ES AC320. This standard works entirely in the loading domain, asking the engineer to prevent connector failure due to tension and shear loading. In this paper, the authors discuss additional criteria related to thermal loading and out-of-plane wind loading that create displacement demand in the non-composite connectors. Loads suitable for such analyses are not well defined. Loads are assumed and demonstrated herein and shown to cause significant displacement demand on connectors. Limited non-composite wythe connector testing is available, and some results are presented here. A comparison indicates that outright failure of non-composite connectors is unlikely for current designs, but fatigue due to thermal and wind loading may be of important consideration, in particular for tall panels.

Keywords: Design Criteria, Non-Composite, Insulated Wall Panels, Thermal Loading, Out-of-Plane Loading, Inter-Wythe Slip.

31 INTRODUCTION

32

33 Sandwich wall panels (SWP) are lately gaining popularity but have been in use for
34 many decades. SWPs typically consist of two layers of concrete, usually termed wythes,
35 separated by a layer of insulation and tied together with connecting elements, often called
36 wythe connectors¹. Engineers often classify SWP in three categories: fully composite, non-
37 composite, and partially composite panels². The only difference between the three categories
38 is the shear transfer capabilities of the wythe connectors. Strong and stiff shear connectors
39 can be used to foster more composite behavior, whereas weaker non-composite wythe
40 connectors are intended not to transfer shear between the wythes.

41 The design of partially and fully composite insulated walls has been the subject of
42 much contemporary research³⁻⁸. The interaction of the layers with composite SWP is
43 complex, but the out-of-plane (OOP) mechanics are generally understood^{5,9}. Further, it is
44 thought that non-composite insulated walls are fairly well understood, though there are no
45 peer reviewed published papers or design codes outlining their mechanics outside of ICC-ES
46 AC320¹⁰ – a semi-codified document that will be discussed in subsequent sections. Non-
47 composite panels follow the same mechanics as partially composite insulated walls, but the
48 connectors cannot transfer as much shear. Most – if not all – engineers simplify the non-
49 composite design to a simple philosophy: the larger wythe carries the design loads, the thin
50 exterior wythe carries little, and make sure the outside wythe does not come off. This
51 philosophy hinges on one, often implicit, assumption: the connectors do not carry shear
52 loading from OOP loads.

53 This paper intends to take a critical look at the way non-composite panels are
54 designed and suggests that additional checks are needed, potentially indicating a height limit
55 may be needed for given connectors and suggesting boundary conditions be controlled.
56 Additionally, while this paper is not able to answer questions about this design, it will raise
57 several questions that the engineering community should consider.

58

59 NON-COMPOSITE MECHANICS

60

61 The following sections form a discussion on the mechanics of non-composite SWP.
62 Currently, AC 320 provides the only guidance outside of proprietary wythe connector
63 suppliers. The AC320 design philosophy is simply to make sure the connectors can hold the
64 dead load of the outer wythe and prevent delamination under the wind suction. The authors
65 argue that the design philosophy should be that the connectors must handle all potential
66 *movement* from environmental and mechanical loading in addition to these loads.

67 DEAD LOAD

68

69 According to AC320, non-composite SWPs are designed to carry the tension and
70 shear loading from their tributary area of the outer wythe as it hangs off of the structural
71 wythe during handling, in addition to service dead load and wind loading acting in tension as
72 seen in Fig. 1 (more discussion on the wind in a later subsection). The equations for this are

73 presented herein. AC320 also provides deformation limits for such (should not exceed 0.1
74 inches under gravity load):

$$\Delta g = \frac{Q_g * d_A^3}{12E_{AB} * I_A} \quad (1)$$

75 Where:

76 Δg = Displacement due to gravity load, inch or mm

77 Q_g = Gravity load on the connector, typically the weight of the fascia layer of the
78 tributary area for the connector

$$d_A = d_d + \frac{2h_v}{3} \left[1 - \frac{1}{1 + h_v/d_d} \right] \quad (2)$$

79 Where:

80 d_A = Connector bending length, a function of insulation thickness and embedment,
81 inch or mm.

82 d_d = Insulation thickness, inch or mm.

83 h_v = Embedment length of the connector in the concrete, inch or mm.

84 E_{AB} = Flexural modulus of elasticity as determined in Section 4.1.3 of AC320¹⁰, psi
85 or Pa.

86 I_A = Moment of Inertia of the connector, in⁴ or mm⁴.

87 Equations (1) and Equation (2), assume a specific type of connector (prismatic beam-like pin
88 connector), but can be modified as needed for a connector of interest by looking up load on a
89 load versus deflection curve, though such approaches are may not endorsed by ICC-ES. The
90 loading is then checked to determine if it satisfies an interaction equation between tension
91 and shear on the connector.

$$\left(\frac{P_s}{P_t} \right) + \left(\frac{V_s}{V_t} \right) \leq 1 \quad (3)$$

92 Where:

93 P_s = Applied service tension load.

94 P_t = Service tension load.

95 V_s = Applied service shear load.

96 V_t = Service shear load.

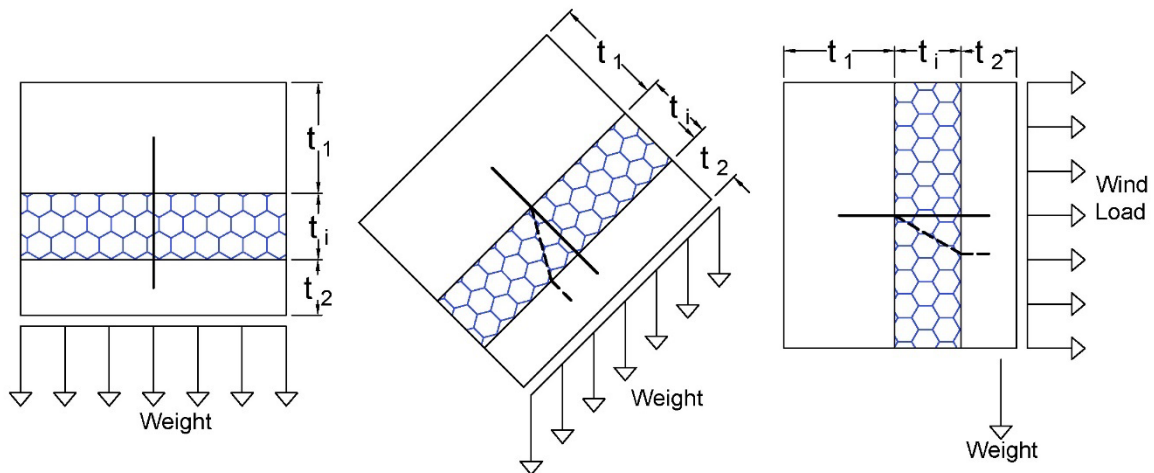


Fig. 1 Actions on wythe connectors discussed in AC320

97

98

99

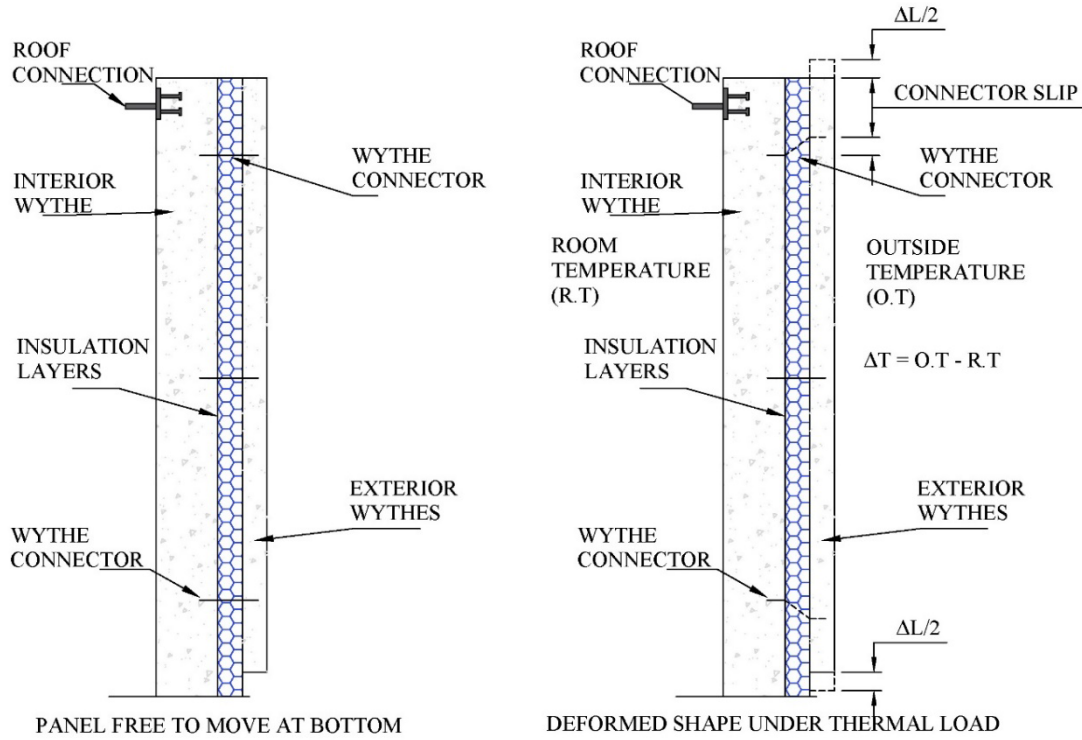
100 THERMAL LOADING

101

102 Non-composite SWPs are usually assumed not to transfer shear load between the two
 103 wythes, which is convenient because resolving these actions can get complex. However, if
 104 one makes this assumption, the connectors must be able to handle the deformations
 105 associated with other actions, particularly thermal loading.

106 Because the interior wythe has heating, ventilation, and air conditioning (HVAC) and
 107 is insulated with a foam layer, the exterior wythe temperature fluctuates, creating a
 108 temperature gradient¹¹. The gradient between these two wythes defines the deformation of
 109 the connectors. On the other hand, the weak and flexible connectors usually employed for
 110 non-composite SWP connectors are assumed to take little or no loading. Because of this
 111 assumption, these thermal deformations are almost completely unrestrained by the
 112 connectors.

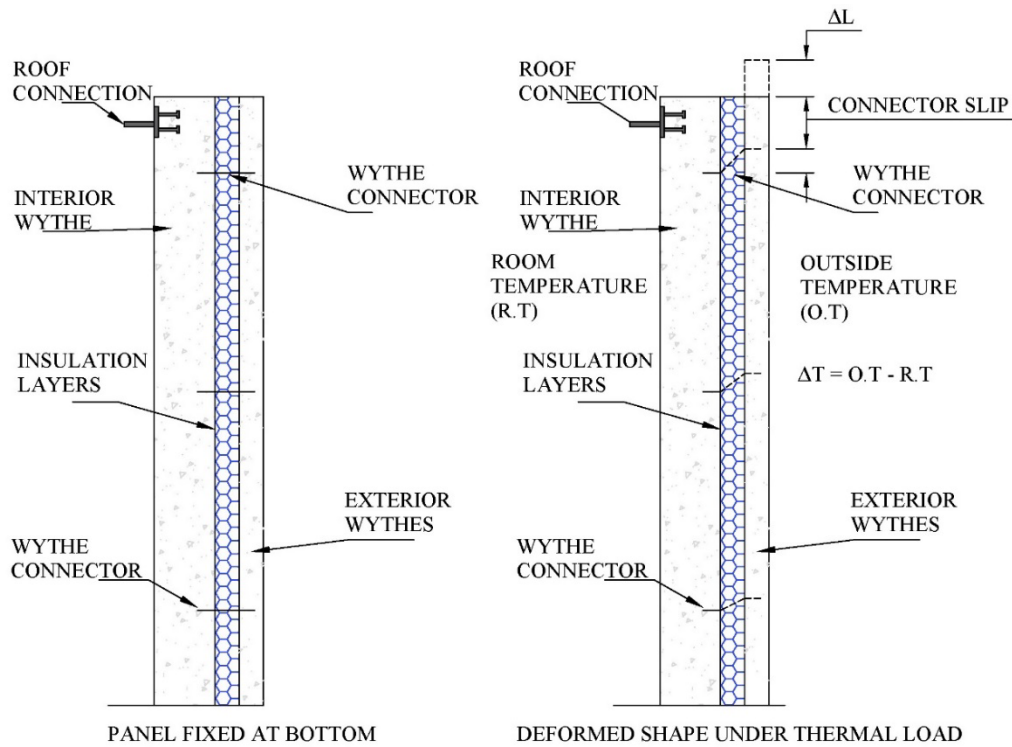
113 If one continues with this assumption, that means the connectors must accommodate
 114 any movement caused by these temperature fluctuations. Ultimately, this deformation must
 115 be checked by the allowable deformation of the connector. Checking such local deformations
 116 of a given connector for a given load is straightforward. Thermal loading and its actions are
 117 demonstrated in Fig. 2 for a boundary condition such that the exterior wythe is floating and
 118 Fig. 3 such that the exterior wythe is grouted. Both boundary conditions exist in practice. In
 119 this case, the most critical connectors are those at the top and/or bottom.



120

121

Fig. 2 Mechanics of SWP Under Thermal Load with Floating Outer Wythe



122

123

Fig. 3 Mechanics of SWP Under Thermal Load with Fixed Outer Wythe

124 To calculate the maximum thermal deformations, familiarity with the mechanics of Equation
125 1 is required. For panels with floating exterior wythes (i.e., ungrouted), the slip in the top and
126 bottom connector locations is half of that calculated by Equation 4 such that the wythe
127 expands about its centerline in both directions. Alternatively, if the bottom is fixed (i.e.,
128 grouted), the deformation is forced vertically. Comparing the two cases, it is clear that these
129 thermal deformations are twice as severe in the latter case.

$$\Delta L = \alpha * L * \Delta T \quad (4)$$

130 Where:

131 α = Coefficient of thermal expansion

132 L = Length of panel

133 ΔT = Temperature change

134 **OUT-OF-PLANE LOADING**

135

136 To simplify the discussion on OOP loading, wind load will be discussed, because
137 seismic loading likely comes with additional concerns, but similar action and kinematics, that
138 will be considered outside the scope of this paper. Further, seismic loading is infrequent
139 when compared to thermal and wind load frequency.

140

141 **WIND LOADING**

142

143 Wind loading is anecdotally not thought to cause any shear load in the connectors;
144 however, this is a false assumption. It is true that the action of wind suction will cause load
145 axial load on a given connector based on its tributary area. However, under OOP wind, the
146 structural wythe will deform in bending, and the exterior wythe (because the connectors keep
147 it attached) must also remain at the same OOP deflection. If this is the case, then the exterior
148 wythe will also have the same curvature and rotation as the structural wythe (this is also the
149 basis for all composite beam theory since Newmark¹²). Provided the connectors can keep the
150 layers in contact, thus meeting this assumption, the rotation of the two wythes will cause
151 shear in the connectors at their connected faces and then actually rotate away from each other
152 (i.e., slip). The mechanics of this deformation is the same as those used for partially
153 composite panels but has been ignored. This local deformation is defined in Fig. 4.

154

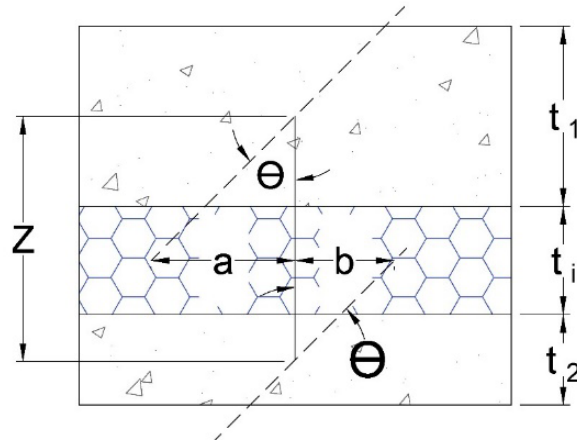


Fig. 4 Relationship Between Rotation and Connector Slip

155
156
157
158
159

Using the relationship in Fig. 4, the slip generated by wythe rotation can be calculated as shown in Equation 5 and Equation 6.

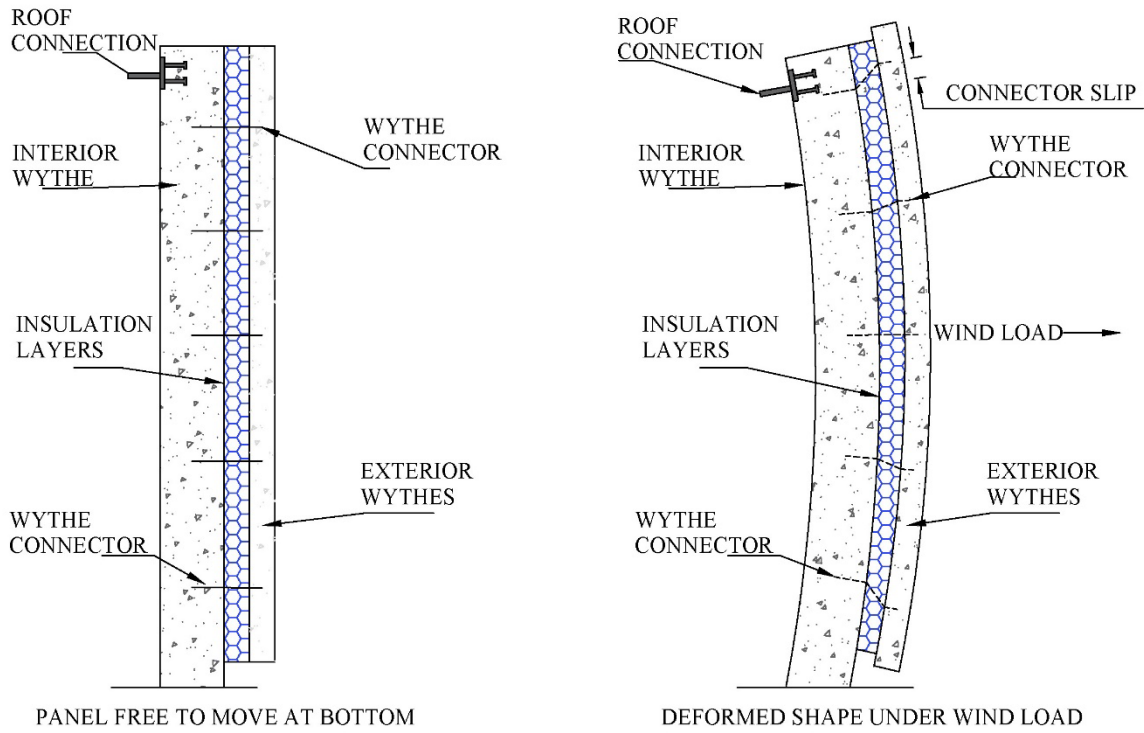
$$\text{Slip} = a + b = \theta * Z \quad (5)$$

$$Z = \frac{t_1}{2} + t_i + \frac{t_2}{2} \quad (6)$$

160 Where:

- 161 θ = Rotation at a connector location
 162 t_1 = Thickness of interior wythe
 163 t_2 = Thickness of exterior wythe
 164 t_i = Thickness of insulation layer
 165 Z = centroidal distance between concrete wythes
 166

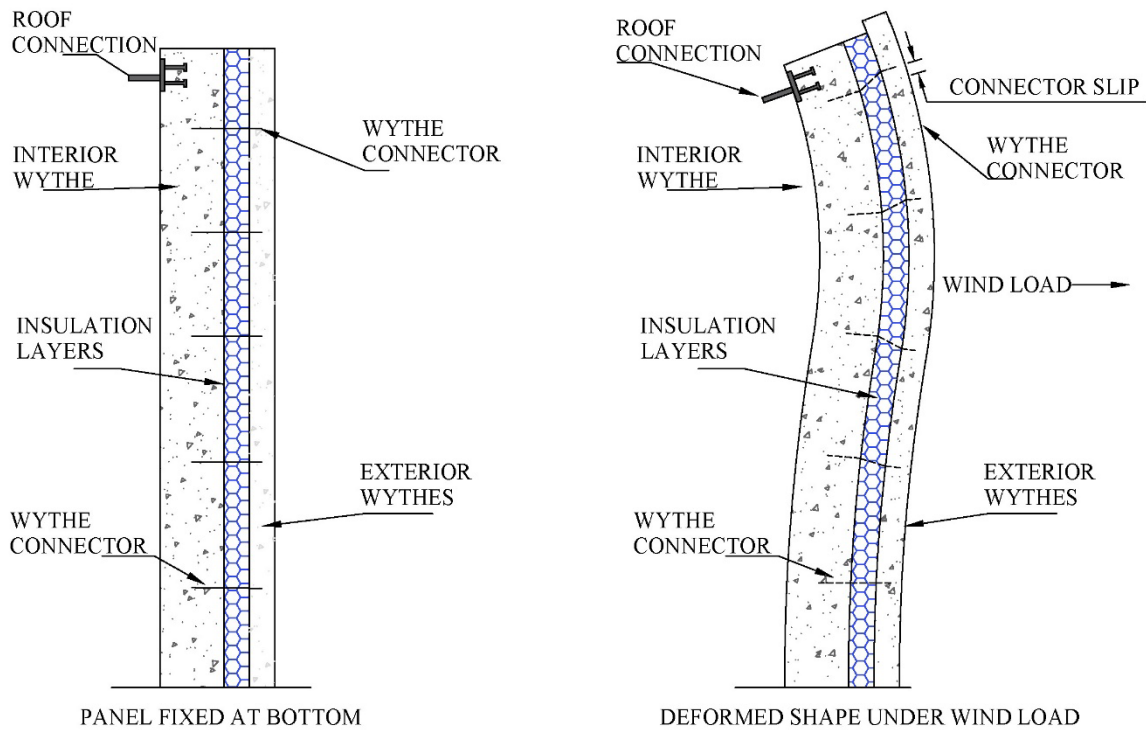
167 The global mechanics of non-composite panels under wind suction load are illustrated
 168 in Fig. 5 and 6 for floating and fixed base conditions, respectively. Clearly, because the slip
 169 follows the rotation of the structural wythe, the critically loaded connectors are the top and
 170 bottom connectors in the floating wythe situation and the top connector in the fixed base
 171 situation.



172

173

Fig. 5 Mechanics of SWP Under Wind Load with Floating Outer Wythe



174

175

Fig. 6 Mechanics of SWP Under Wind Load with Fixed Outer Wythe

176

To calculate the slip at a connector location due to bending of the panel under uniform wind load, the rotation (θ) is calculated using Equation 7 for the floating wythe condition and using Equation 8 for the fixed-pin connection. Fig. 4 illustrates the relationship between the rotation and slip in the connector, and Equations 5 and 6 (fundamental beam mechanics) are used to calculate the connector slip using the calculated rotation.

177

178

179

180

$$\theta(x) = \frac{-w}{24EI} (L^3 - 6L * x^2 + 4x^3) \tag{7}$$

$$\theta(x) = \frac{-w * x}{48EI} (6L^2 - 15L * x + 8x^2) \tag{8}$$

181

Where:

182

θ = Rotation

183

w = Wind load

184

L = Length of panel

185

x = location along the panel

186

E = Modulus of elasticity

187

I = Moment of inertia of the *structural wythe*

188

189 One will notice that these are fundamental relationships familiar to all structural engineers,
190 not complex sandwich theory^{13,14}. The use of sandwich theory would produce similar
191 answers but is not straightforward. Just like the discussion on thermal loading, because the
192 connectors are assumed to be very flexible and weak, they cannot restrain this OOP bending.
193 Therefore, the important consideration is that the connectors can handle the deformations
194 imposed by this action.
195

196 **LOADS**

197

198 Even though the mechanics outlined above are easy to identify and implement,
199 determining the loading that is appropriate and for which scenarios are not. The effect of
200 diurnal and annual temperature swings on the mechanical performance of insulated wall
201 panels is not known. The sun comes up daily, causing at least 18,250 temperature cycles of
202 variable magnitude. The difference between the maximum and minimum temperatures in a
203 year is very large. The magnitude of the thermal gradient is likely related to solar radiation,
204 the thermal mass of the structure, ambient temperatures, and exterior convection.

205 The effects of wind are better understood. The design loading in ASCE 7-16 is a 700-
206 year load, but there are equations to reduce this to a different return period, and the hazard
207 tool provides several wind velocities for different return periods. Loads of consequence are
208 likely infrequent during wind events but depending on the state of the panel (cracked, or
209 uncracked), the slip generated could be significant.

210

211

212 **TEMPERATURE LOADING**

213

214 To illustrate temperature loads, three cities were selected to represent hot, cold, and
215 moderate areas. These cities were Phoenix, Arizona; Grand Forks, North Dakota; and
216 Omaha, Nebraska, to represent hot, cold, and moderate, respectively. Temperature data were
217 obtained from the National Oceanic and Atmospheric Administration¹⁵ for the past 50 years
218 for each location. The maximum and minimum daily temperatures were plotted, from which
219 the average daily temperature swing and yearly temperature swing were calculated, as shown
220 in Fig. 7. These temperatures are air temperatures only and are used as surrogates for
221 concrete temperature because such loads are unknown. These air temperatures are used only
222 to provide an estimate and context for the forthcoming analyses. The temperature swing is
223 reported, rather than the gradient (internal minus external temperature changes) because if
224 the internal wythe is thermally stationary, the exterior wythe will expand and contract
225 independently, and these swings will result in repeated deformations of the connectors.

226 The yearly probability for 20 deg. F and 40 deg. F daily changes are reported in Table 1(a)
227 for context. The temperature swing histograms for all three cities can be seen in Fig. 8.
228 Seasonal temperature swings are another infrequent, but certain, cyclic temperature load. For
229 the purposes of this discussion, this is considered the difference between the maximum and
230 minimum temperature values for one year. Such a temperature change will require the non-
231 composite connectors to accommodate these wythe deformations. Table 2 shows the average

232 seasonal temperature swing for the three cities. Fig. 7 illustrates an example of a daily and
 233 seasonal temperature swing for the city of Omaha for 2021 only.

234

235 Table 1 Average daily temperature swings

City	Average Temp. Swing (ΔT) F	Standard Deviation (σ) F	Probability of $\Delta T > 20$ F	Probability of $\Delta T > 40$ F
Phoenix	24.02	5.91	75.2%	0.34%
Grand Forks	20.06	9.13	50.3%	1.45%
Omaha	21.41	8.68	56.5%	1.62%

236

237 Table 2 Seasonal temperature swings

238

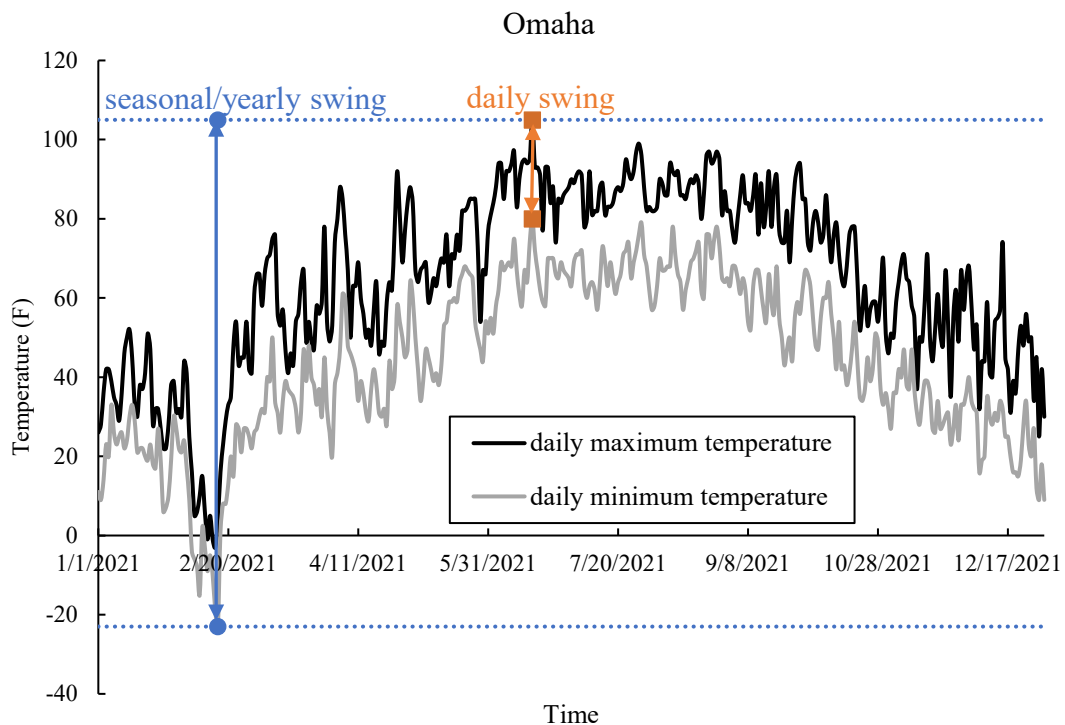
239

240

241

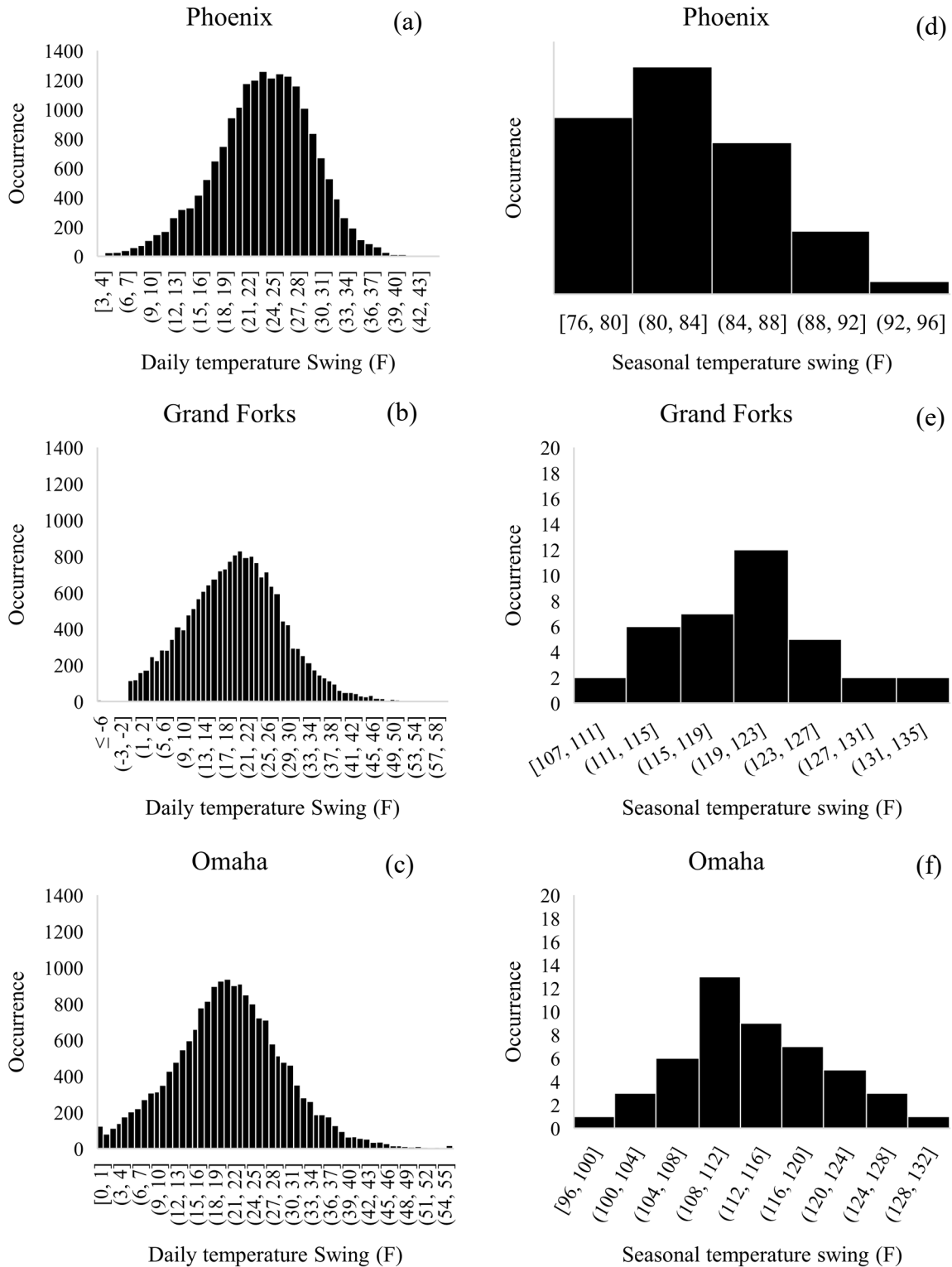
242

City	Average Yearly Temp. Swing (ΔT) F	Standard Deviation (σ) F
Phoenix	83.1	4.27
Grand Forks	120	6.26
Omaha	114	7.41



243

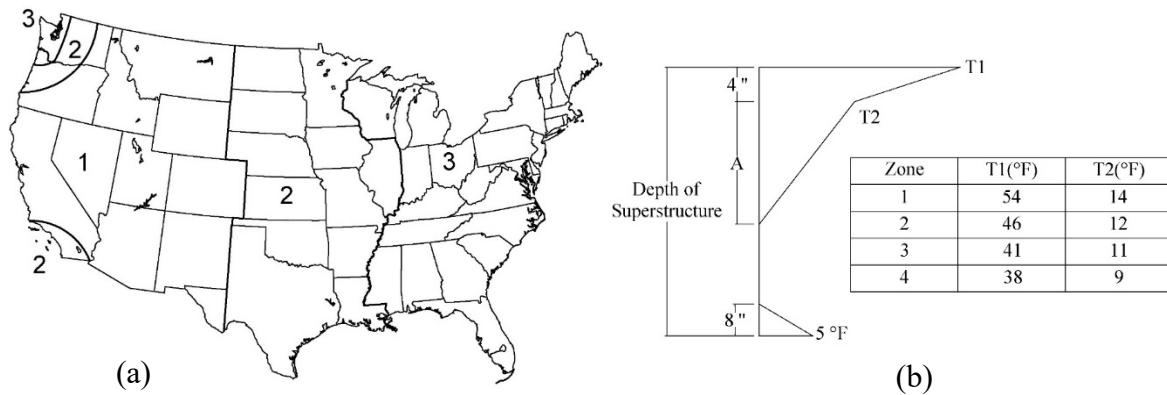
244 Fig. 7 Example of seasonal and daily swing for Omaha city



245 Fig. 8 Daily (a), (b), and (c) and seasonal (d), (e), and (f) temperature swing histograms for
 246 Phoenix, Grand Forks, and Omaha

247 These temperatures are ambient temperatures and only illustrative. Actual
 248 temperature gradients are unknown as there are no experimental programs that have collected
 249 such data for insulated walls. The AASHTO LRFD¹⁶ bridge design specification provides a
 250 design model for the thermal gradient. The model divides the United States map into four
 251 zones of solar radiation, see Fig. 9 (a), and used two lines from the top of the girder and one
 252 straight line from the bottom, as seen in figure Fig. 9 (b), which has shown to be accurate for
 253 box girder bridges¹⁷, but it is unlikely to be accurate for SWP. A similar approach could be
 254 undertaken for SWP, which would have implications for both non-composite and composite
 255 SWP designs.

256



257

258

Fig. 9 (a) Solar radiation zones (b) updated vertical design gradient¹⁶.

259

260 The gradients shown in the AASHTO LRFD code (Fig. 9 b) are higher than those
 261 implied by Fig. 8, likely because ambient temperature swings are not the same as thermal
 262 gradients and the concrete retains thermal energy due to its thermal mass as ambient
 263 temperatures change. Further, the temperature gradients in SWP are likely higher than those
 264 in a bridge because of the wall insulation and the HVAC regulating temperatures of the
 265 interior wythe.

266

267 WIND LOADING

268

269 In contrast to temperature loads, wind is clearly stated and quantified in the ASCE 7-
 270 16¹⁸. For the purposes of this analyses, the ASCE Hazard Tool was used to determine sub-
 271 design recurrence interval loading and example loads are presented in Table 3 for the three
 272 locations above. To calculate the pressure from wind speed, ASCE 7 provides the following
 273 equation 9 assuming the K coefficients are set to 1.0 for simplicity.

$$q_z = 0.00256 * V^2 \text{ (lb/ft}^2\text{)} \tag{9}$$

274

275

276 Where:

277 $V = \text{wind speed (mph)}$

278

279 The average 10-year and 50-year loads were 14.66 (lb/ft²) and 21.24 (lb/ft²),
280 respectively and not appreciably different between locations studied in this manuscript.

281

282 Table 3 Wind speeds and loads for the three cities

Location	10-year wind speed (mph)	50-year wind speed (mph)	10-year wind load (lb/ft ²)	50-year wind load (lb/ft ²)
Omaha	77	90	15.18	20.74
Phoenix	75	96	14.40	23.59
Grand Forks	75	87	14.40	19.38
Average	76	91	14.66	21.24

283

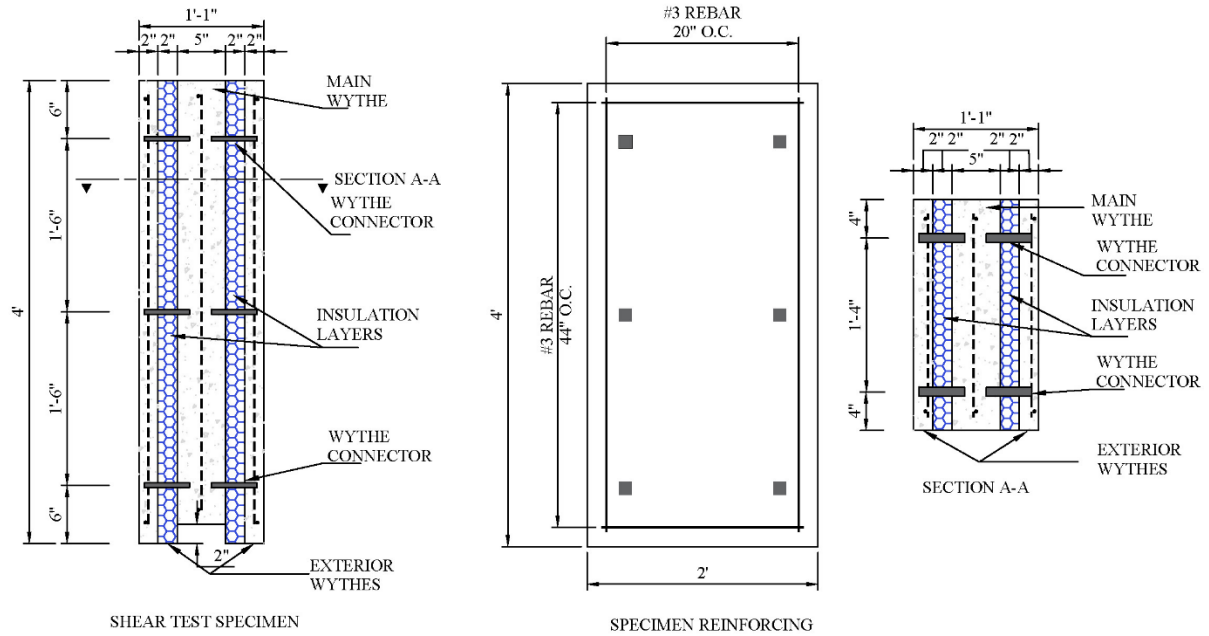
284 WYTHE CONNECTORS

285

286 In the preceding section, the actions of different loads were described. AC320
287 describes means of testing non-composite wythe connectors (based on ASTM E488-09) but
288 only requires the reporting of their static strength. Except for the dead load tension and shear
289 and wind load tension, the slips generated from thermal and wind do not necessarily test the
290 strength of the connector. Rather, the OOP bending and thermal mechanics require that a
291 non-composite connector be flexible and accommodate deformations that are otherwise
292 unrestrained. If such deformations exceed the deformation capability of a given connector, it
293 will likely fail, and the exterior wythe delaminate.

294 Because of the lack of data on such connectors, a total of six double-shear specimens
295 were tested to quantify the shear load vs displacement behavior for the non-composite
296 connectors following the procedure outline in reference ¹⁹. This testing was only performed
297 to provide a point of reference for this paper, so the connector itself is only described as a
298 common, proprietary, non-composite connector.

299 The specimens were double shear type specimens²⁰ with dimensions of 4 ft by 2 ft
300 and consisted of three layers of concrete separated by two layers of foam. Both outer
301 concrete wythes were 2 in. while the inner concrete wythe was 5 in. The insulated foam
302 layers were composed of two 1-in. thick XPS foam sheets to ensure no insulation
303 contribution to the shear strength and provide a debonded plane. Two different arrangements
304 of connectors were used for each group of three double-shear specimens to determine if there
305 were any differences in specimen configuration. The first group had four connectors
306 connecting the exterior wythe to the central wythe wythes, a total of eight for the entire
307 specimen, while the second group had six connectors connecting the exterior wythe to the
308 central wythe, with a total of twelve connectors. The six-connector version is shown in Fig.
309 10; the four-connector version was identical, except the center row of connectors was
310 removed.



311

312

Fig. 10 Typical double shear specimen

313

314

315

316

317

318

A hydraulic ram was used to apply the load concentric to the inner concrete wythe. The load was measured using a 100-kip load cell. The two outer wythes were supported by the load frame while the inner wythe was free to move as shown in Fig. 11. The relative movement of the inner wythe was measured as the average of four total string potentiometers placed on the mid-height of the specimen. After sensor installation, the specimen was loaded until complete separation of the wythes.

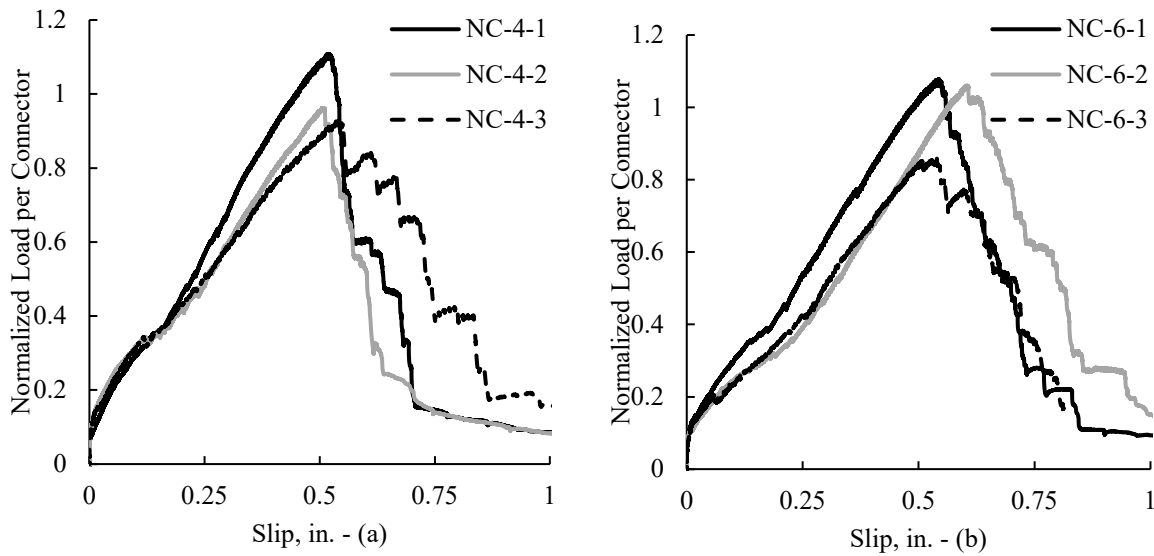


319

320

Fig. 11 Double shear specimen test setup

321 Fig. 12 presents the load versus deformation curves for the two types of specimens.
 322 Specimens were labeled NC-[number of connectors per exterior wythe]-[iteration number].
 323 The NC-4 series specimens and the NC-6 series specimens generally had the same near-
 324 linear behavior following what looked like an early vertical line attributed to breakaway
 325 friction of the insulation layers. Table 3 presents the normalized maximum strength and the
 326 slip at maximum strength for each of the six total tests. The strength of the connector was
 327 normalized by the average of all six tests to obscure which connector was tested, further, the
 328 load is superfluous to the discussion. These results indicate the two configurations were
 329 functionally identical. The average slip at maximum for these connectors was 0.544 in.
 330



331 Fig. 12 Load vs slip results for (a) four connectors per wythe and (b) six connectors per
 332 wythe

333
 334

Table 4 Double shear results

Specimen	Maximum Normalized Load per Connector	Slip at Max Strength (in.)
NC-4-1	1.11	0.521
NC-4-2	0.96	0.506
NC-4-3	0.93	0.546
NC-6-1	1.08	0.544
NC-6-2	1.06	0.606
NC-6-3	0.859	0.539
Average	1.00	0.544

335

336 In the context of the subsection preceding this one, the connectors need to
 337 accommodate movement of the wythes relative to each other as well as the in-place loads
 338 like the localized wind loading from their tributary area and the shear dead load. It seems that
 339 in the case of this connector, the displacements should not exceed 0.544 in. or the connector
 340 will fail.

341 Unfortunately, there is little information on cyclic testing of such connectors. It is
 342 unknown how repeated wind and thermal cycles will affect connector performance long
 343 term. AC320 has no guidance on this but does provide a cyclic testing regime geared toward
 344 seismic capacity as shown in Table 4, but not deformation capacity or hysteretic behavior. In
 345 reality the total number of cycles due to wind and thermal is not well understood, but based
 346 on the histograms of Fig. 8, the loads and number of cycles will not be reflected by the
 347 seismic cycles in Table 4.

348

349 Table 5 AC320 Shear cyclic load regime

Load Level	Number of cycles
$\pm V_s$	10
$\pm V_i$	30
$\pm V_m$	100

350 Where: V_i = A load midway between V_s and V_m , V_m = One-fourth the average ultimate shear load, V_{ref} , in concrete of the tested strength,
 351 V_s = The maximum shear test load.

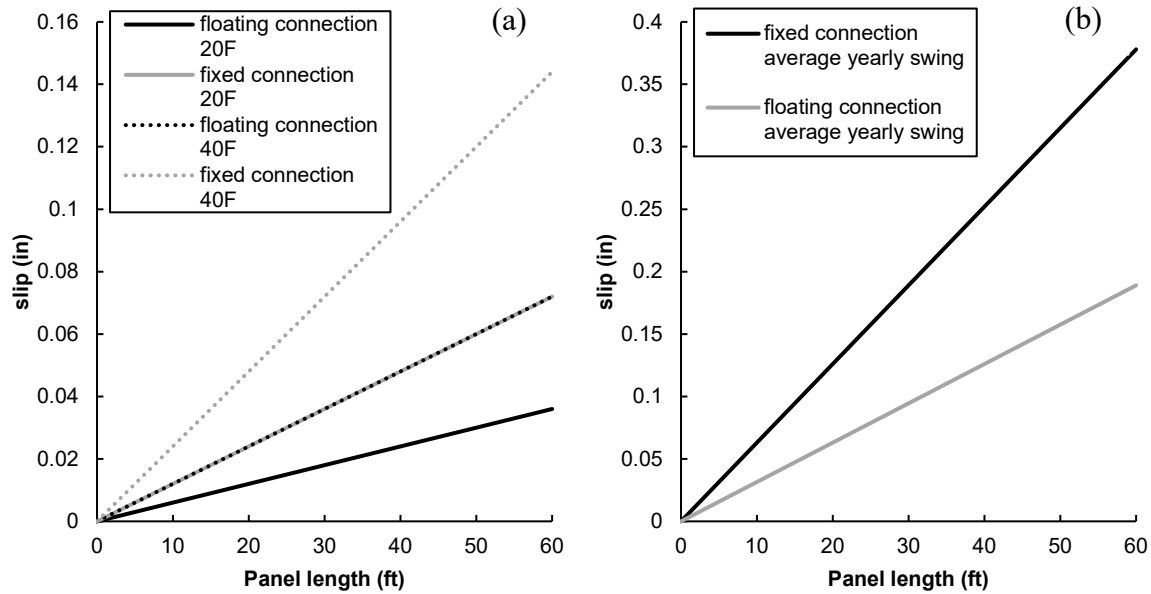
352

353 DISCUSSION

354

355 The above discussions about loading and slip calculations have been separated into
 356 this section, but the intent is to combine this information to determine if, with the best
 357 available knowledge, there should be changes to the way precast engineers think about non-
 358 composite SWP connector design.

359 Calculating the slip due to thermal loads requires an estimate of wythe temperatures,
 360 panel length, and coefficient of thermal expansion of the concrete (CTE). The CTE is
 361 estimated between 4.1 and 7.3 microstrain/degF²¹ and for the analyses here is taken as 5
 362 microstrain/degF. In lieu of better data, thermal swings of 20°F and 40°F for the floating and
 363 the fixed exterior wythe conditions are plotted for different panel heights up to 60 ft in. The
 364 best practice of keeping the exterior wythe floating keeps these low thermal swings minimal,
 365 but such slips are significant.

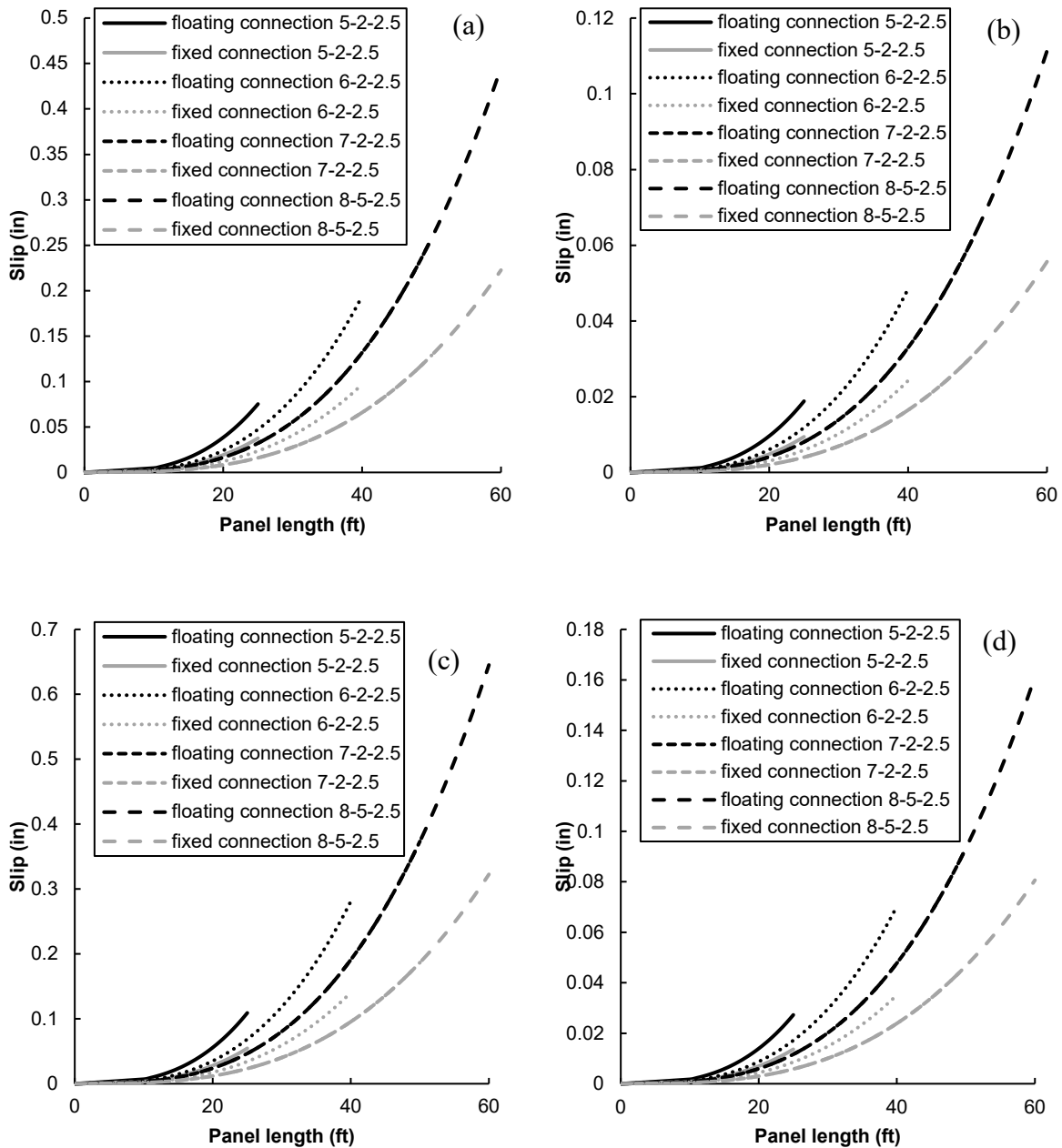


366

367 Fig. 13 (a) Slip vs panel length for floating and fixed connection for 20°F and 40°F (a) Slip
 368 vs panel length for floating and fixed connection for average yearly swing of three cities

369 Considering the displacement capabilities outlined in Table 3, such loads may
 370 approach displacements that will cause significant damage to the connector reducing its
 371 capacity over time. It seems that the temperature changes on the order of daily swings may
 372 only pose issues for larger panel heights and connectors that may not have the ductility of
 373 those tested here. However, the yearly temperature swings illustrated in Fig. 13b are very
 374 large and could limit the use of non-composite connectors at taller heights. At a minimum,
 375 such displacements would likely cause some damage, lowering the connector tensile and
 376 shear capacity. As contemporary panels continue to increase in height, this issue may well
 377 become exacerbated as the temperature slip is linearly related to the panel height.

378 Considering the mechanics under wind load described above, the slip for SWP
 379 varying in length from 10 ft to 60 ft was calculated for different structural wythe and
 380 insulation thicknesses. The calculation was done for an uncracked panel as well as a cracked
 381 panel (using $I_{cr} = 0.25 \cdot I_g$ per ACI 318²² Section 6.6.3.1.1 for simplicity, though this could
 382 overestimate I_{cr} in a slender panel). Loads applied were 14.7 psf (10-year wind) and 21.2 psf
 383 (50-year), which a panel would be expected to resist at least five times and one time during
 384 its anticipated lifespan. The nomenclature x-y-z was used to represent the thickness of the
 385 interior wythe, insulation, and exterior wythe for x, y, and z, respectively. In Fig. 14, the slip
 386 was calculated for both floating and fixed end conditions with an insulation thickness of 2
 387 inches and an interior wythe thickness of 5, 6, 7 and 8 inches for both cracked and uncracked
 388 panels. Because the slip is related to the thickness of the panel, as well as the rotation (a
 389 function of the height cubed) very large slips are shown.



390 Fig. 14 Slip vs panel length for floating and fixed connection with 2-inch insulation under
 391 wind load for (a) cracked panel and 14.66 (lb/ft²) load (b) uncracked panel and 14.66 (lb/ft²)
 392 load (c) cracked panel and 21.24 (lb/ft²) load (d) uncracked panel and 21.24 (lb/ft²) load

393 While the wind loading at the above rate is not a very frequent event, this illustrates
 394 the importance understanding the slip capabilities of the connectors to be designed. If the
 395 connector slip capacity is 0.5 in. (per the tests herein) a 10-year wind event may well result in
 396 ruptured connectors and delamination in cracked panels. For uncracked panels, this slip at
 397 these loads is much smaller and may only contribute to possible strength reduction of the

398 connector discussed in the thermal section. Such fatigue information is not widely available.
399 For the 50-year wind events, induced slips are also very large, and assuming a cracked panel,
400 has the potential to fail the connectors for tall panels. Further, if non-composite panel
401 connectors are expected to remain intact under failure conditions like ultimate loads, where
402 the fully cracked section properties are expected, it is unlikely that a connector with such
403 displacement capacity can remain intact and are likely to fail prior to the nominal capacity of
404 the member.

405 The purpose of the above discussion is to talk about the fundamental kinematics of
406 the panels and get engineers to think about potential limits on connectors, particularly in
407 taller panels. There is limited information available on displacement capacity and fatigue
408 performance of in-service non-composite connectors, but the very limited testing program
409 here indicates that issues are unlikely for the panel heights considered. Regardless, the
410 mechanics discussed herein should become part of a formalized design document so as to
411 determine if issues may arise in future designs as panel heights continue to go up.

412 CONCLUSIONS

413

414 This paper has discussed the design of connectors for non-composite panels. The
415 ICC-ES AC308 document outlines the testing and design of such connectors, but works only
416 in the load domain, rather than the displacement domain. Displacement demand from thermal
417 and wind loading was discussed and the mechanics for calculating connector displacement
418 demand was presented. Loads were introduced and discussed, in particular their
419 shortcomings and future needs. Using the mechanics and assumed loads, connector
420 displacement demand was calculated and presented. The results indicated large connector
421 slip displacements may be large enough to cause fatigue and performance drop. However,
422 there is such limited information on connector data, it is difficult to quantify these effects.
423 This paper has generated more questions than answers, but the following conclusions can be
424 made regarding the discussion above:

- 425
- 426 • The mechanics of thermal and OOP load-induced connector slip are relatively
427 easy to implement and familiar to most engineers.
 - 428 • There is limited guidance on thermal loading for SWPs, and this paper calls
429 for additional study of thermal gradient loading in SWPs. This has
430 implications in both non-composite and composite SWP.
 - 431 • Connector slip from thermal and OOP loading is highly dependent on the
432 length of the panel, and connectors in taller panels may experience issues with
433 slip demand.
 - 434 • Slip demand from thermal and OOP wind loading may cause fatigue in non-
435 composite connectors in SWP, reducing their capacity, particularly in taller
436 panels. There is no available data on this currently.

436

437 **REFERENCES**

438

- 439 1. Maguire M, Pozo-Lora FF. Partially Composite Concrete Sandwich Wall Panels.
440 *Concrete International*. 2020;42(10):47-52.
441 [https://www.concrete.org/publications/internationalconcreteabstractsportal.aspx?m=de](https://www.concrete.org/publications/internationalconcreteabstractsportal.aspx?m=details&ID=51728201)
442 [tails&ID=51728201](https://www.concrete.org/publications/internationalconcreteabstractsportal.aspx?m=details&ID=51728201)
- 443 2. Amin Einea PE, Salmon DC, Fogarasi GJ, Culp TD, Tadros MK. State-of-the-art of
444 precast concrete sandwich panels. *PCI journal*. 1991;36(6):78-98.
- 445 3. Salam AR, Taylor S, Marc M. Iterative and Simplified Sandwich Beam Theory for
446 Partially Composite Concrete Sandwich Wall Panels. *Journal of Structural*
447 *Engineering*. 2021;147(10):04021143. doi:10.1061/(ASCE)ST.1943-541X.0003116
- 448 4. Al-Rubaye S, Sorensen T, Thomas RJ, Maguire M. Generalized beam-spring model
449 for predicting elastic behavior of partially composite concrete sandwich wall panels.
450 *Eng Struct*. 2019;198:109533. doi:10.1016/J.ENGSTRUCT.2019.109533
- 451 5. Jensen K, Al-Rubaye S, Thomas RJ, Maguire M. Mechanics-Based model for elastic
452 Bending, Axial, thermal Deformations, and asymmetry of concrete composite
453 sandwich wall panels. *Structures*. 2020;23:459-471.
454 doi:10.1016/J.ISTRUC.2019.11.004
- 455 6. Gombeda MJ, Trasborg P, Naito CJ, Quiel SE. Simplified model for partially-
456 composite precast concrete insulated wall panels subjected to lateral loading. *Eng*
457 *Struct*. 2017;138:367-380. doi:10.1016/J.ENGSTRUCT.2017.01.065
- 458 7. Frankl BA, Lucier GW, Hassan TK, Rizkalla SH. Behavior of precast, prestressed
459 concrete sandwich wall panels reinforced with CFRP shear grid. *PCI journal*.
460 2011;56(2):42-54.
- 461 8. Cox B, Syndergaard P, Al-Rubaye S, Pozo-Lora FF, Tawadrous R, Maguire M.
462 Lumped GFRP star connector system for partial composite action in insulated precast
463 concrete sandwich panels. *Compos Struct*. 2019;229:111465.
464 doi:10.1016/j.compstruct.2019.111465
- 465 9. Pozo-Lora FF, Maguire M. Flexural Behavior of Continuous Non-Loadbearing
466 Insulated Wall Panels. In: *2019 PCI/NBC*. PCI; 2019:15.
- 467 10. International Code Council Evaluation Service (ICC-ES). *Acceptance Criteria for*
468 *Fiber-Reinforced Polymer Composite or Unreinforced Polymer Connectors Anchored*
469 *in Concrete, AC308*. ; 2015.
- 470 11. Pozo-Lora F, Maguire M. Thermal bowing of concrete sandwich panels with flexible
471 shear connectors. *Journal of Building Engineering*. 2020;29:101124.
472 doi:10.1016/j.jobbe.2019.101124
- 473 12. Newmark NM. Test and analysis of composite beams with incomplete interaction.
474 *Proceedings of society for experimental stress analysis*. 1951;9(1):75-92.

- 475 13. Holmberg A, Plem E. *Behaviour of Load-Bearing Sandwich-Type Structures*.
476 Bygghorsknigen; 1965.
- 477 14. Granholm H. *Om Sammansatta Balkar Och Pelare Med Särskild Hänsyn till Spikade*
478 *Träkonstruktioner: On Composite Beams and Columns with Particular Regard to*
479 *Nailed Timber Structures*. Vol 17. Gumpert; 1949.
- 480 15. National Oceanic and Atmospheric Administration. NOAA.
- 481 16. Knovel (Firm), AASHTO. *AASHTO LRFD Bridge Design Specifications, Customary*
482 *U.S. Units.*; 2012.
- 483 17. Marc M, Carin RW, Tommy C. Live-Load Testing and Long-Term Monitoring of the
484 Varina-Enon Bridge: Investigating Thermal Distress. *Journal of Bridge Engineering*.
485 2018;23(3):04018003. doi:10.1061/(ASCE)BE.1943-5592.0001200
- 486 18. ASCE/SEI. *Minimum Design Loads and Associated Criteria for Buildings and Other*
487 *Structures*. ASCE/SEI 7-16. American Society of Civil Engineers; 2017.
488 doi:10.1061/9780784414248
- 489 19. Pozo-Lora FF, Maguire M. Determination of the Mechanical Properties of Flexible
490 Connectors for Use in Insulated Concrete Wall Panels. *JoVE*. 2022;(188):e64292.
491 doi:doi:10.3791/64292
- 492 20. Syndergaard P. Comparing sandwich wall panel shear connector testing
493 methodologies. Published online 2018.
- 494 21. Federal Highway Administration Research and Technology, Portland Cement
495 Concrete Pavements Research. *Thermal Coefficient Of Portland Cement Concrete.*;
496 2016.
- 497 22. 318 ACIC. 318-19(22): Building Code Requirements for Structural Concrete and
498 Commentary (Reapproved 2022). *Technical Documents*.
- 499
- 500